

Ly α Blobs as an Observational Signature of Cold Accretion Streams into Galaxies

Mark Dijkstra* and Abraham Loeb

¹*Astronomy Department, Harvard University, 60 Garden Street, Cambridge, MA 02138, USA*

31 October 2018

ABSTRACT

Recent hydrodynamic simulations of galaxy formation reveal streams of cold ($T \sim 10^4$ K) gas flowing into the centers of dark matter halos as massive as $10^{12-13.5} M_{\odot}$ at redshifts $z \sim 1-3$. In this paper we show that if $\gtrsim 20\%$ of the gravitational binding energy of the gas is radiated away, then the simulated cold flows are spatially extended Ly α sources with luminosities, Ly α line widths, and number densities that are comparable to those of observed Ly α blobs. Furthermore, the filamentary structure of the cold flows can explain the wide range of observed Ly α blob morphologies. Since the most massive halos form in dense environments, the association of Ly α blobs with overdense regions arise naturally. We argue that Ly α blobs - even those which are clearly associated with starburst galaxies or quasars - provide direct observational support for the cold accretion mode of galaxies. We discuss various testable predictions of this association.

Key words: cosmology: theory–galaxies: haloes–galaxies: formation–galaxies: cooling flows–galaxies: intergalactic medium–line: formation

1 INTRODUCTION

The physical origin of spatially extended Ly α sources, also known as Ly α blobs (LABs), is still enatic. LABs have been associated with cooling radiation, in which gas that collapses inside a host dark matter halo releases a significant fraction of its gravitational binding energy in Ly α line emission (Haiman et al. 2000; Fardal et al. 2001; Birnboim & Dekel 2003; Dijkstra et al. 2006, also see Katz & Gunn 1991). Other mechanism that have been invoked to explain the origin of LABs include: photoionization of cold ($T \sim 10^4$ K), dense, spatially extended gas by obscured quasars (Haiman & Rees 2001; Geach et al. 2009), population III stars (Jimenez & Haiman 2006), or spatially extended inverse Compton X-ray emission (Scharf et al. 2003); the compression of ambient gas by superwinds into dense, cold Ly α emitting shells (e.g. Taniguchi & Shioya 2000; Mori et al. 2004); or star formation that is triggered by relativistic jets (Rees 1989); or some combination of photoionization and cooling (Furlanetto et al. 2005).

Since their discovery by Steidel et al. (2000, also see Keel et al. 1999), several tens of new LABs have been found (e.g. Matsuda et al. 2004; Dey et al. 2005; Saito et al. 2006; Smith et al. 2009). These are typically associated with massive halos that reside in dense parts of the Universe (Steidel et al. 2000; Matsuda et al. 2004, 2006). Multi-

wavelength studies of Ly α blobs have revealed a clear association of the brighter blobs with regular Lyman Break galaxies (LBGs, e.g. Matsuda et al. 2004), sub-millimeter (sub-mm) and infrared (IR) sources which imply star formation rates of $\sim 10^3 M_{\odot} \text{ yr}^{-1}$ (Chapman et al. 2001; Geach et al. 2005, 2007; Matsuda et al. 2007), or with unobscured (Bunker et al. 2003; Weidinger et al. 2004) and obscured quasars (Basu-Zych & Scharf 2004; Geach et al. 2007; Smith et al. 2009). However, in other blobs this association has been ruled out, which has led to the conclusion that cooling radiation by cold accreting gas may have been observed (Nilsson et al. 2006; Matsuda et al. 2006; Saito et al. 2008; Smith & Jarvis 2007; Smith et al. 2008a).

We propose that the sources that are associated with the Ly α blobs may have little to do in powering the spatially extended Ly α emission. This proposal is physically motivated by recent hydrodynamical simulations of galaxy formation, which show that baryons assemble into galaxies through a two-phase medium which contains filamentary streams of cold ($T \sim 10^4$ K) gas embedded within a hot gaseous halo (e.g. Kereš et al. 2005; Dekel & Birnboim 2006; Ocvirk et al. 2008; Dekel et al. 2009; Kereš et al. 2009; Agertz et al. 2009). The cold flows contain $\sim 5-50\%$ of the total gas content (Birnboim et al. 2007; Kereš et al. 2009) in halos with masses in the range $M_{\text{halo}} \sim 10^{12-10^{13.5}} M_{\odot}$ (Dekel et al. 2009). As we will show in this paper, these cold streams are probable sources of spatially extended Ly α emission. Under very reasonable assumptions we find that

* E-mail:mdijkstra@cfa.harvard.edu

the cold accretion model ‘predicts’ the existence of spatially extended Ly α sources with properties reminiscent of the observed LABs around massive halos ($M_{\text{halo}} \gtrsim 10^{12} M_{\odot}$).

The outline of this paper is as follows: we describe our model in § 2. In § 3 we present our results, before discussing our work in § 4 and presenting our conclusions in § 5. The cosmological parameter values used throughout our discussion are $(\Omega_m, \Omega_{\Lambda}, \Omega_b, h, \sigma_8) = (0.27, 0.73, 0.046, 0.70, 0.82)$ (Komatsu et al. 2009), and we denote the primordial helium abundance by mass as $Y_{\text{He}} = 0.24$ (e.g. Izotov et al. 1997).

2 THE MODEL

Our model is based on the scenario for cold accretion that has emerged from recent simulations (Kereš et al. 2009). ‘Hot’ gas that is in hydrostatic equilibrium with the dark matter potential well at the virial temperature of the dark matter halo is in pressure equilibrium with the cold gas (also see Fall & Rees 1985; Rees 1989), which makes up a fraction f_{cold} of the total gas mass of the halo, M_{gas} . We further assume that the gas mass fraction, f_{gas} , is half of the universal value. Hence, the total gas mass $M_{\text{gas}} \equiv f_{\text{gas}} M_{\text{halo}} = 0.5\Omega_b/\Omega_M M_{\text{halo}} = 0.08M_{\text{halo}}$. This accounts for a substantial fraction of baryons that may be locked up in (dwarf) galaxies that reside within the halo of interest. The assumed gas mass fraction $f_{\text{gas}} = 0.08$ is in good agreement with the value derived for groups of galaxies at $z < 1$ (e.g. Giodini et al. 2009). As the cold streams navigate to the center of their host dark matter halo, they are progressively heated by the release of a fraction of their gravitational potential energy through weak shocks (Rees & Ostriker 1977; Haiman & Rees 2001). This heating of the cold gas is balanced by radiative cooling, mostly through the Ly α emission line. Next, we describe the model in more detail.

- We use the gas density profile for hot gas that is in hydrostatic equilibrium with an NFW (Navarro et al. 1997) dark matter potential well with a concentration parameter $c = 3.8$ (Gao et al. 2008) at the virial temperature of the halo as derived by Makino et al (1998, their Eqs. 8 and 11). This profile is very similar to an isothermal β -model, which – according to the simulations – provides an accurate description of the hot gas component (Kereš et al. 2009). In § 4.6 we show that our final results are robust against variations in the assumed density profile.

- The hot gas reaches the virial temperature, $T_{\text{h}}(r) = T_{\text{vir}} = 1.9 \times 10^6 \text{K} (M_{\text{halo}}/10^{12} M_{\odot})^{2/3} [(1+z)/4]$, and co-exists in pressure equilibrium with the cold gas. Pressure equilibrium between the hot (‘h’) and cold (‘c’) gas implies that $n_{\text{c}}(r)T_{\text{c}}(r) = n_{\text{h}}(r)T_{\text{h}}(r)$, in which $n(r)$ and $T(r)$ denote the number density of particles and the gas temperature, respectively. We obtain $T_{\text{c}}(r)$ under the assumption that cooling balances the heating of the cold flows that occurs as they navigate into the center of the dark matter halo.

We parametrize the gravitational heating rate by assuming that a fraction f_{grav} (f_{hot}) of the change in the gravitational potential energy of each gas element along its trajectory is converted into heat in the cold (hot) gas. The remaining fraction $(1 - f_{\text{grav}} - f_{\text{hot}})$ is converted into additional kinetic energy of the gas element. Throughout the paper, we assume that the transfer of energy into the hot gas is negligible, i.e. $f_{\text{hot}} = 0$. This assumption appears reasonable

given that the majority of the cold gas mass is in smooth continuous streams (Kereš et al. 2009; Dekel et al. 2009), as opposed to discrete clouds which are likely to heat the hot gas (e.g. Dekel & Birnboim 2008, and references therein). Under this assumption, which is discussed in more detail in § 4.6.2, $f_{\text{grav}} = 1$ corresponds to infall at a constant velocity, while $f_{\text{grav}} = 0$ corresponds to free-fall.

For the sake of simplicity, we adopt the conservative working assumption of a constant non-zero f_{grav} inside the virial radius (r_{vir}) of galaxy halos and $f_{\text{grav}} = 0$ outside. The most recent Smoothed Particle Hydrodynamical (SPH) simulations (Kereš et al. 2009) indicate that the cold flows propagate inward at an approximately constant speed, implying $f_{\text{grav}} \sim 1$; however, Adaptive Mesh Refinement (AMR) simulations (Ocvirk et al. 2008; Dekel et al. 2009) indicate that the cold gas accelerates throughout its motion and that therefore f_{grav} may be smaller¹. Future simulations might be able to refine our working assumption by resolving the precise dynamics and heating of the cold flows. Hence, the heating rate per particle is given by

$$H(r) = f_{\text{grav}} \times \frac{GM(<r)\mu m_p}{r^2} v(r) + H_{\gamma}(r), \quad (1)$$

where μ is the mean molecular weight per particle in the cold flow (in units of m_p), and $v(r)$ denotes the infall velocity which is given

$$v^2(r) = 2v^2(r_{\text{vir}}) + 2(1 - f_{\text{grav}} - f_{\text{hot}}) \int_{r_{\text{vir}}}^r ds \frac{GM(<s)}{s^2}, \quad (2)$$

and we assume that $v(r_{\text{vir}}) = \sqrt{2}v_{\text{circ}}$ (with our results not being sensitive to this choice). The term $H_{\gamma}(r)$ denotes the heating rate due to absorption of ionizing radiation. At the typical densities in the cold flows ($n_{\text{c}} \gtrsim 0.1 \text{ cm}^{-3}$) the gas is self-shielded from external ionizing radiation, and hence $H_{\gamma}(r) = 0$. It is possible however, that galaxies embedded within the cold flow may photoionize some surrounding region which would locally boost $H(r)$ (Furlanetto et al. 2005). In any case, ignoring this extra photoheating term only makes our predicted Ly α luminosities from the cold flows smaller, and therefore makes our results more conservative. As was mentioned above, we assume that $f_{\text{hot}} = 0$.

We obtain an equilibrium temperature $T_{\text{c}}(r)$ at radius r by equating $H(r)$ to the cooling rate per particle in the cold flow, which is given by,

$$\Lambda(r, T, x_{\text{HI}}) = \frac{1}{n_{\text{c}}} [n_{\text{e}} n_{\text{HI}} C_{\text{cool}}(T_{\text{c}}) + n_{\text{e}} n_{\text{HII}} R_{\text{cool}}(T_{\text{c}})]. \quad (3)$$

Here, the first term in the square brackets denotes the cooling rate (in $\text{erg s}^{-1} \text{ cm}^{-3}$) due to collisional excitation of H atoms by electrons. The second term denotes the cooling rate due to recombination events of free electrons and protons (other cooling processes are negligibly small for the typical gas temperature in the cold flow). The rate coefficients $C_{\text{cool}}(T_{\text{c}})$ and $R_{\text{cool}}(T_{\text{c}})$ were taken from Hui & Gnedin (1997, hereafter HG97). Finally, the ionization state of the gas determines its cooling rate. Under the

¹ Our discussion focuses on the extended Ly α emission, and not on the compact core of the galaxy where the cold streams are finally brought to rest. Note that dust may suppress the Ly α luminosity from the core, but is less likely to affect the cold streams which carry metal-poor intergalactic gas.

assumption that the gas is self-shielding (which is justified later) we obtain a one-to-one relation between T and x_{HI} through $x_{\text{HI}} = \alpha_{\text{rec,B}}(T_c)/(\alpha_{\text{rec,B}}(T_c) + C_{\text{ion}}(T_c))$. Here, $C_{\text{ion}}(T_c)$ denotes the collisional ionization rate coefficient, and $\alpha_{\text{rec,B}}(T_c)$ denotes the case-B recombination coefficient (as the cold neutral gas is optically thick in all Lyman-series lines and case-B applies; the related coefficients were taken from HG97). At the temperatures of interest, helium is neutral inside the cold gas and free electrons are only supplied by hydrogen, i.e. $n_{\text{HI}}(r) = x_{\text{HI}}(r)n_c(r)/[1 + (Y_{\text{He}}/4)]$ and $n_{\text{HII}}(r) = n_e(r) = [1 - x_{\text{HI}}(r)]n_c(r)/[1 + (Y_{\text{He}}/4)]$.

In practice we assume that $T_c = 10^4$ K and compute n_c assuming pressure equilibrium. Since temperature determines the ionization state of the gas in self-shielded gas, we obtain a cooling rate which we compare to the heating rate. If $\Lambda(r, T, x_{\text{HI}}) > H(r)$ ($\Lambda(r, T, x_{\text{HI}}) < H(r)$), then T_c is lowered (increased) until the cooling and heating rates are equal to within 1%.

- Once the temperature, density and ionization state of the gas have been determined, we compute the Ly α emissivity (in $\text{erg s}^{-1} \text{cm}^{-3}$) as a function of radius,

$$\epsilon_{\text{Ly}\alpha}(r) = n_e n_{\text{HI}} C_{\text{Ly}\alpha}(T_c) + 0.68 h\nu_{\alpha} n_e n_{\text{HII}} \alpha_{\text{rec,B}}(T_c). \quad (4)$$

Here, the first term denotes the luminosity density in Ly α photons (in $\text{erg s}^{-1} \text{cm}^{-3}$) following collisional excitation of H atoms by free electrons. The collisional excitation coefficient is given by $C_{\text{Ly}\alpha} = 3.7 \times 10^{-17} \exp(-h\nu_{\alpha}/kT)/T^{1/2} \text{erg s}^{-1} \text{cm}^3$ (Osterbrock 1989, p 55). The second term denotes the luminosity density in Ly α photons following case-B recombination, and that $\sim 68\%$ of all case-B recombination events result (Osterbrock 1989) in a Ly α photon of energy $h\nu_{\alpha} = 10.2$ eV. In practice, the recombination term can be safely ignored.

- Lastly, we obtain the total Ly α luminosity by integrating over volume, namely

$$L_{\text{Ly}\alpha} = \mathcal{T}_{\alpha} \int_0^{r_{\text{vir}}} dr 4\pi r^2 \epsilon_{\text{Ly}\alpha}(r) f_{\text{cold}} \frac{T_c(r)}{T_{\text{h}}}. \quad (5)$$

Emission from $r > r_{\text{vir}}$ is expected to have a surface brightness that is well below the detection threshold of existing observations, because beyond r_{vir} no rarefied hot gas exists to confine the cold flow (Kereš et al. 2009; Dekel et al. 2009), and so the cold gas density declines considerably. The gas at $r > r_{\text{vir}}$ therefore provides a negligible contribution to the total Ly α luminosity. The fraction f_{cold} (which we assume to be independent of radius) is taken from Figure 3 of Kereš et al. (2009), which we parametrize as $f_{\text{cold}} = 0.25(M_{\text{halo}}/10^{12} M_{\odot})^{-0.55}$ for $M_{\text{halo}} \leq 4 \times 10^{13} M_{\odot}$, and $f_{\text{cold}} = 0$ otherwise. Furthermore, \mathcal{T}_{α} denotes the fraction of Ly α that makes it to the observer. The factor $f_{\text{cold}} T_c(r)/T_{\text{h}}$ in the integrand denotes the fraction of the volume that is occupied by the cold gas in the range of radii within $r \pm dr/2$.

3 RESULTS

Throughout the paper we assume that $f_{\text{grav}} = 0.3$, which we regard as a conservative choice (see § 2 for a more detailed discussion). Furthermore, we assume that $\mathcal{T}_{\alpha} = 0.5$. That is, $\sim 50\%$ of the emitted Ly α photons is observed. The most likely source of opacity is provided by residual HI in

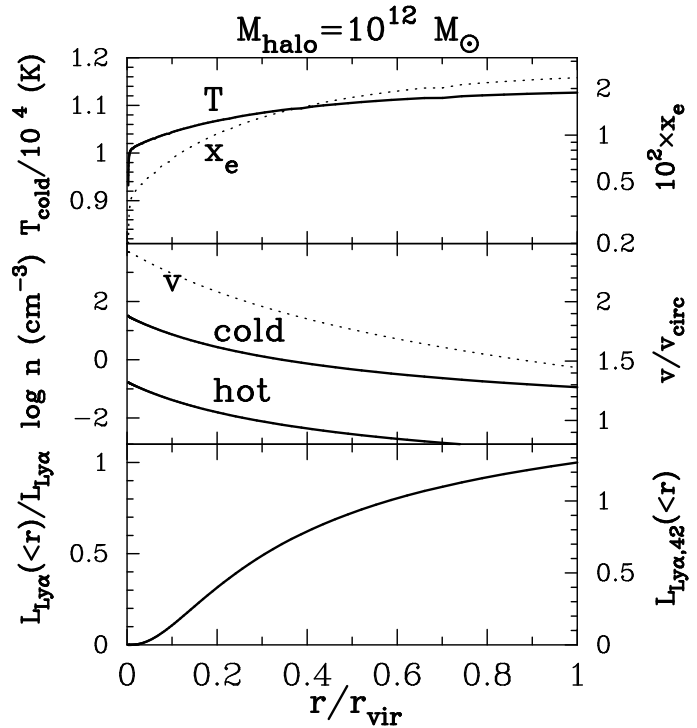


Figure 1. *Top panel:* the *solid* and *dotted* lines show the radial dependence of the temperature and electron fraction by number of the cold gas phase for a dark matter halo of mass $M_{\text{halo}} = 10^{12} M_{\odot}$, and under the assumption that a fraction $f_{\text{grav}} = 0.3$ of the gravitational binding energy of the gas is converted into heat. *Central panel:* the *solid* lines show the number densities of gas particles in the cold and hot phase and the *dotted* line shows the infall velocity of the gas expressed in units of v_{circ} . *Bottom panel:* the fraction of Ly α luminosity that is emitted interior to a radius r (normalized by the total, $L_{\alpha,\text{tot}} \approx 1.3 \times 10^{42} \text{erg s}^{-1}$).

the intergalactic medium (IGM), which mostly affects the flux of photons that was emitted blueward of the Ly α resonance (e.g Fig 3 of Madau 1995). At $z = 2$, $z = 3$ and $z = 4$, the mean transmitted fraction of photons emitted blueward of the Ly α resonance is $\langle \mathcal{T}_{\alpha} \rangle \sim 0.8$, $\langle \mathcal{T}_{\alpha} \rangle \sim 0.7$, and $\langle \mathcal{T}_{\alpha} \rangle \sim 0.4$, respectively (e.g. Faucher-Giguère et al. 2008b). However, these fractions apply to an average that was taken over a scales of tens of comoving Mpc (cMpc) along the line of sight. Since the massive halos of interest reside in dense parts of the Universe, we expect the local to be more opaque than average (e.g. Dijkstra et al. 2007; Dijkstra 2009), which motivates our choice $\mathcal{T}_{\alpha} = 0.5$ at $z \leq 3$. The gas in the cold flows consists mainly of compressed neutral intergalactic gas and dust opacity is likely negligible (see § 4.2 for additional discussion on dust).

3.1 The Halo Mass-Ly α Luminosity Correlation

Consider a halo of mass $M_{\text{halo}} = 10^{12} M_{\odot}$, for which $v_{\text{circ}} = 220 \text{ km s}^{-1}$, $T_{\text{vir}} = 1.9 \times 10^6 \text{ K}$, and $r_{\text{vir}} = 82 \text{ kpc}$ (see, e.g. Barkana & Loeb 2001, their Eqs. 24-26). The *solid line* in the *top panel* of Figure 1 shows the radial dependence of the gas temperature in the cold flow. The *dotted line* shows the electron fraction by number, i.e. $x_e = x_{\text{HII}} = n_{\text{HII}}/n_p$, where n_p denotes the number density of protons. The temperature is found to be in the narrow range of $\sim 1-1.1 \times 10^4 \text{ K}$ which

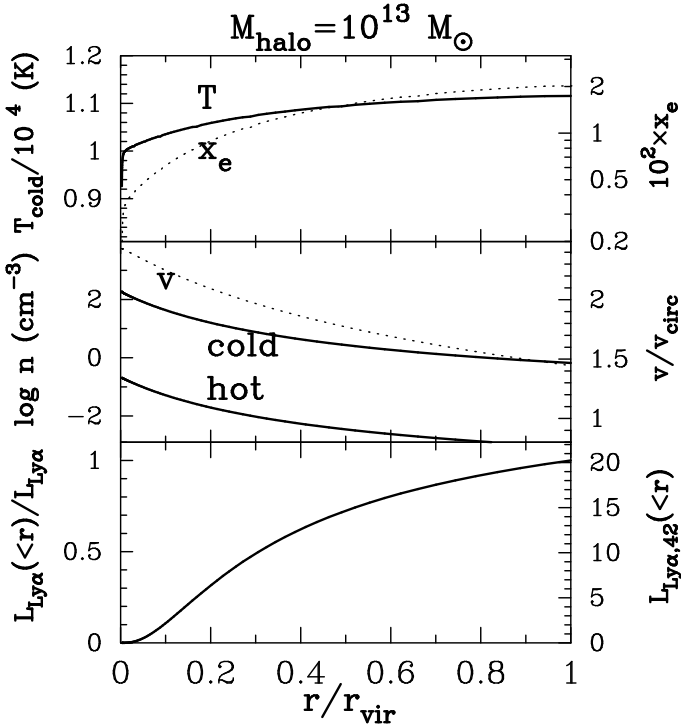


Figure 2. Same as Fig 1, but for a dark matter halo of mass $M_{\text{halo}} = 10^{13} M_{\odot}$.

results in a very low level of ionization ($x_e \sim 10^{-2}$). This is caused by the fact that atomic line cooling is very efficient at the densities encountered in the cold flow (see *central panel*), and so the gas cools down to the temperature floor below which collisional line excitation is ineffective. The temperature and ionization fraction increase outward as the density, and therefore the cooling rate decreases with radius. Figure 2 shows the same quantities for a halo of mass $M_{\text{halo}} = 10^{13} M_{\odot}$.

The *solid lines* in the *central panels* shows the number densities of gas particles in both the cold and hot phase. The *dotted line* shows the infall velocity in units of v_{circ} . (Note that the infall velocity enters the heating rate through Eq. 1.) The cold gas is denser by a factor of T_{vir}/T_c . This results in number densities in the cold phase that exceed $1-10 \text{ cm}^{-3}$ at $r \lesssim 0.5r_{\text{vir}}$. These high densities justify our assumption of self-shielding: the recombination rate in the cold flow is $\alpha_{\text{rec}} n_c \sim 10^{-11} - 10^{-12} \text{ s}^{-1}$, while the photoionization rate by the UV background in the IGM at $z = 3$ is $\Gamma_{\text{UV}} \approx 6 \times 10^{-13} \text{ s}^{-1}$ (e.g Faucher-Giguère et al. 2008a). Even the gas on the very edge of the cold flow, that is optically thin to ionizing background, contains an ionized fraction of hydrogen (by number) of only $x_{\text{HI}} = 1 + \frac{a}{2} - \frac{1}{2}(a^2 + 4a)^{1/2}$, where $a \equiv \Gamma_{\text{UV}}/n_c \alpha_{\text{rec}}$. Therefore, $x_{\text{HI}} = 0.2 - 0.6$ for $n_c = 1 - 10 \text{ cm}^{-3}$. That is, even this gas is significantly neutral, and the gas becomes self-shielding less than a pc into the flow. Note that boosting the local photoionization rate by a factor of 10^2 does not change this conclusion².

² Because in our model the Ly α blobs are associated with massive halos, $M_{\text{halo}} > 10^{12} M_{\odot}$, the cold filaments are compressed by a factor of $(T_{\text{vir}}/10^4 \text{ K}) \gtrsim 200(M_{\text{halo}}/10^{12} M_{\odot})^{2/3}$ by the hot virialized gas. Therefore the gas in our model is denser and better

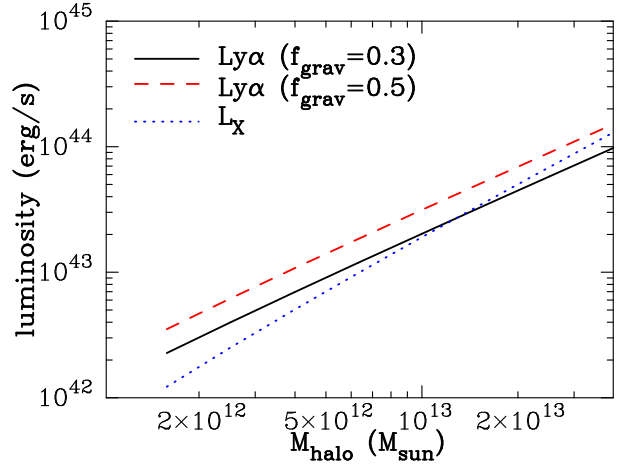


Figure 3. The *solid line* shows the dependence of the total Ly α luminosity as a function of halo mass, M_{halo} , when a fraction f_{grav} of the gravitational binding energy of the cold gas is converted into heat. This model predicts Ly α luminosities in the range $10^{42} - 10^{44} \text{ erg s}^{-1}$ (comparable to the range of values observed from the majority of blobs, see Matsuda et al 2004) for halo masses in the range $M_{\text{halo}} = 10^{12} - 3 \times 10^{13} M_{\odot}$. To explain the luminosity of the most luminous ($L_{\text{Ly}\alpha} = 10^{44} \text{ erg s}^{-1}$) blob with cold accretion requires a halo of mass $M_{\text{halo}} \sim 3 \times 10^{13} M_{\odot}$, close to the maximum halo mass that can host cold flows (DeKel et al. 2009). The *blue dotted line* shows the soft X-ray (free-free) luminosity of the hot gas. There are not nearly enough X-rays to significantly boost the Ly α emissivity of the cold flows (see text).

The *lower panel* shows the total Ly α luminosity that was emitted interior to radius r (normalized to the total, which is $L_{\alpha, \text{tot}} \approx 2 \times 10^{43} \text{ erg s}^{-1}$). We find that $\sim 50\%$ of all Ly α is emitted at $r \gtrsim 0.3r_{\text{vir}}$. Hence, our total calculated Ly α luminosity is emitted over a spatially extended region. It is not possible to robustly predict the surface brightness profile as this is determined by the number of filaments in the cold flow, their geometry and their orientation relative to the observer. The surface brightness profile would furthermore be sensitive to any radial dependence of the ‘gravitational heating efficiency’-parameter f_{grav} .

Figure 3 shows the dependence of the total Ly α luminosity, $L_{\text{Ly}\alpha}$, as a function of halo mass, M_{halo} as the *solid line*. We find Ly α luminosities in the range $10^{42} - 10^{43} \text{ erg s}^{-1}$, comparable to the observed range in LABs (Matsuda et al. 2004) for halo masses in the range $M_{\text{halo}} = 10^{12} - 10^{13} M_{\odot}$. In order to obtain $L_{\text{Ly}\alpha} = 10^{44} \text{ erg s}^{-1}$, which is the luminosity of the brightest of blobs that was found by Steidel et al. (2000), we either need a halo with a mass of $\sim 3 \times 10^{13} M_{\odot}$, or a somewhat lower halo mass with a higher f_{grav} .

The *blue dotted line* shows the total X-ray luminosity of the hot phase which is given by,

$$L_X = \int_0^{r_{\text{vir}}} dr 4\pi r^2 n_e(r) n_{\text{HII}}(r) (1 + Y_{\text{He}}) \epsilon_{\text{ff}}(T_{\text{vir}}), \quad (6)$$

where $\epsilon_{\text{ff}}(T_{\text{vir}}) = 1.4 \times 10^{-27} T^{1/2} \text{ erg s}^{-1} \text{ cm}^3$ is the free-

capable of self shielding than in the models of Furlanetto et al. (2005). For this reason, the photoionizing background is not dominating the heating – and resultant Ly α cooling – rate from the cold flows

free emissivity (see e.g. Eq 5.15b of Rybicki & Lightman 1979). Note that the hot gas is fully ionized with $n_{\text{HII}}(r) = n_h(r)/(2 + \frac{3}{4}Y_{\text{He}})$, and an electron density $n_e = (1 + \frac{1}{2}Y_{\text{He}})n_{\text{HII}}$.

The X-ray luminosity is comparable to the Ly α luminosity. One may think that the X-rays can penetrate the cold flows and boost the Ly α luminosity. This is unlikely the case, as the frequency dependence of the free-free spectrum is given by $L_{\nu,ff} \propto \exp(-h_p\nu/kT_h)$, and therefore the hot gas emits photons as energetic as $h_p\nu \sim 0.5(T_{\text{vir}}/5 \times 10^6 \text{ K}) \text{ keV}$. These soft X-ray photons easily penetrate deep into the cold flows where they photoionize either hydrogen or helium atoms, and create an energetic electron. In a neutral medium, $\sim 40\%$ of the energy of the electron goes into exciting HI, $\sim 30\%$ goes into collisionally ionizing HI, and $\sim 10\%$ goes into heating the gas (the rest excites and ionizes helium, Shull & Van Steenberg 1985). Hence, even if the cold flows absorb all X-rays, line excitation by secondary electrons would only boost the Ly α emissivity by at most a factor of $\lesssim 1.4$. Furthermore, a boost in the ionization (and thus electron) fraction naively boosts atomic line cooling rate – and hence Ly α emissivity – by the same factor. However, even if X-rays (significantly) enhance the electron fraction in the cold flow, the cooling at a given temperature would only be more efficient so as to balance the heating rate. Since at most 10% of the X-ray energy is converted into heat, this heating rate is boosted by a factor $\lesssim 1.1$. The above estimates assume that the cold flows absorb *all* the X-rays; this is very unlikely to occur in reality because the cold medium occupies a fraction $\sim f_{\text{cold}}T_c/T_h \sim 10^{-4} - 10^{-3}$ of the volume of the halo, and the majority of X-rays freely escape out from the halo. The boost in Ly α emissivity from the cold flows due to X-rays is therefore negligible. The X-ray photons that escape would redshift to energies $h_p\nu \lesssim 0.125(T_{\text{vir}}/5 \times 10^6 \text{ K}) \text{ keV}$, and would not be detectable with existing X-ray telescopes. Note however, that metals can boost the X-ray emissivity of the hot gas at energies $\gg 1 \text{ keV}$. Deep X-ray observations may therefore set useful limits on the amount of hot gas in the dark matter halos hosting the blobs (as in Geach et al. 2009, who put an upper limit on the average mass of halos hosting Ly α blobs of $M_{\text{halo}} < 10^{13}M_{\odot}$), although these limits do depend on the assumed metallicity of the hot gas.

3.2 The Ly α Luminosity Function of Cold-Accretion Powered Blobs

The previously obtained relation between galaxy mass and Ly α luminosity allows us to compute a luminosity function of accretion powered LABs from the mass function of dark matter halos. Observed LABs are known to be associated with a region that contain a significant overdensities of Lyman-break galaxies (LBGs) with a fractional excess density of $\delta_{\text{LBC}} = 5.0 \pm 1.2$ (Steidel et al. 1998, 2003). It is essential to take into account this overdensity when predicting the expected number density of LABs brighter than L_{α} as (Barkana & Loeb 2004),

$$n_{\text{blob}}(> L_{\alpha}; \delta_M(V_s)) = \int_{M_{\text{min}}(L_{\alpha})}^{\infty} dm \frac{dn_{\text{ST}}}{dm} B(m, \delta_M(V_s)), \quad (7)$$

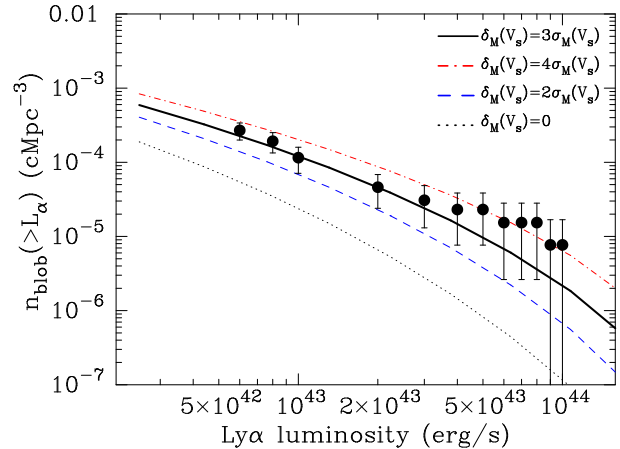


Figure 4. The *solid line* shows the number density of Ly α blobs brighter than L_{α} , $n_{\text{blob}}(> L_{\alpha}) \text{ cMpc}^{-3}$, and taking into account that fractional overdensity of the region of the Universe in which the blobs reside is $\delta_M(V_s) = 3\sigma_M(V_s)$. The *dashed* and *dotted* line refer to values of $\delta_M(V_s) = 2\sigma_M(V_s)$ and $\delta_M(V_s) = 5\sigma_M(V_s)$, bracketing the likely range of overdensities inferred from the observed overdensity of LBGs in the region by Steidel et al. (1998). Here, $\sigma_M^2(V_s)$ denotes the variance of the density field averaged over spheres of volume $V_s = 1.3 \times 10^5 \text{ cMpc}^3$ (the survey volume). Our model with $f_{\text{grav}} = 0.3$ provides a good fit to the data. The present uncertainty on $\delta_M(V_s)$ allows models with $f_{\text{grav}} \gtrsim 0.15$ to reproduce the observed number of Ly α blobs. The *black dotted line* shows the number of blobs expected in an ‘average’ part (i.e. $\delta_M(V_s) = 0$) of the Universe, indicating how rare the most luminous blobs are ($n_{\text{blob}}(> 10^{44} \text{ erg s}^{-1}) \sim 10^{-7} \text{ cMpc}^{-3}$).

where $(dn_{\text{ST}}/dm)dm$ denotes the Sheth-Tormen number density of dark matter halos (in cMpc^{-3} , Sheth & Tormen 1999) in the mass range $M_{\text{halo}} = m \pm dm/2$. The factor $B(m, \delta_M(V_s))$ denotes the boost in the number of halos due to the overall matter overdensity, $\delta_M(V_s)$, within the survey volume V_s .

In Figure 4 we plot $n_{\text{blob}}(> L_{\alpha}; \delta_M(V_s))$ as a function of Ly α luminosity for three values of the overdensity $\delta_M(V_s) = 2\sigma_M(V_s)$ (*dashed line*), $3\sigma_M(V_s)$ (*solid line*), and $4\sigma_M(V_s)$ (*red dotted line*). Here, $\sigma_M^2(V_s) = 0.013$ denotes the variance in the matter density field at $z = 3$ averaged over spheres of the survey comoving volume $V_s = 1.3 \times 10^5 \text{ cMpc}^3$. The overdensities $\delta_M(V_s)$ were chosen so as to reproduce the observed boost and standard deviation in the LBG number density, under the assumption that LBGs are associated with dark matter halos of mass $M_{\text{halo}} = 10^{12}M_{\odot}$ (see Appendix A).

The data points were derived by taking the ratio between the number of blobs (Matsuda et al. 2004) brighter than L_{α} and the survey volume $V_s = 1.3 \times 10^5 \text{ cMpc}^3$. The error bars on the data points were obtained from the relation $\sigma^2 = b^2\sigma_M^2(V_s) + \sigma_P^2$, where σ_P denotes the Poisson error and $b^2\sigma_M^2(V_s)$ denotes the cosmic variance for a bias factor $b = b(M_{\text{halo}}, z)$, which is in turn calculated following Somerville et al. (2004). For the cumulative luminosity function, the errors were added in quadrature.

Figure 4 shows that the model luminosity function agrees well with the data (Matsuda et al. 2004). The uncertainty in $\delta_M(V_s)$ allows for a large spread in the predicted $n_{\text{blob}}(> L_{\alpha})$, especially at the bright end. This is because the most massive ($M_{\text{halo}} \sim 10^{13}M_{\odot}$) halos are highly bi-

ased tracers of the mass and their number density depends sensitively on $\delta_M(V_s)$. The sensitivity of the cumulative luminosity function to $\delta_M(V_s)$ implies that good fits to the data are possible for a range of gravitational heating efficiencies, f_{grav} . In the allowed range between $\delta_M(V_s) = 2\sigma_M(V_s)$ and $4\sigma_M(V_s)$, we obtain a good fit for $f_{\text{grav}} > 0.15$. Our predicted number of Ly α blobs is practically degenerate in the product $\mathcal{T}_\alpha \times f_{\text{grav}}$, and this constraint can be recast as $\mathcal{T}_\alpha f_{\text{grav}} \gtrsim 0.075$. Therefore, only a relatively low gravitational heating efficiency suffices to make the cold flows ‘glow’ in Ly α at luminosities observed from the Ly α blobs.

Lastly, the *black dotted line* in Figure 4 shows the number density of blobs expected in an ‘average’ part (i.e. $\delta_M(V_s) = 0$) of the Universe. This implies that the most luminous blobs that were originally discovered by Steidel et al (2000), are significantly rarer in the field (where $n_{\text{blob}}(> 10^{44} \text{ erg s}^{-1}) \sim 10^{-7} \text{ cMpc}^{-3}$). Our prediction is consistent with a recent upper limit of $n_{\text{blob}}(L_\alpha > 10^{44} \text{ erg s}^{-1}) \lesssim 5 \times 10^{-7} \text{ cMpc}^{-3}$ (Yang et al. 2009).

4 DISCUSSION

4.1 Predicted Ly α Blobs Spectral Line Shapes and Physical Sizes

The typical velocity widths (FWHM) of the LABs span the range (Matsuda et al. 2006) of 500–1700 km s $^{-1}$. In the cold-accretion model, infall occurs at velocities in the range 1.0–2.5 $v_{\text{circ}} \sim 220$ –1500 km s $^{-1}$, which naturally result in the observed velocity widths (taking into account projection effects due to the orientation of the filaments, and the intergalactic absorption that suppresses the observed flux of the ‘bluest’ Ly α photons (e.g. Madau 1995)). Although the gas in the cold flows is mostly neutral, resonant scattering is not expected to broaden the Ly α line beyond the observed velocity widths of the blobs, as we discuss next.

The cold flows are highly elongated structures, and the majority of the Ly α photons escape in a direction perpendicular to the axis of the flow. Therefore, at the densities of interest the Ly α photons have to traverse an HI column density $N_{\text{HI}} \sim 10^{21} - 10^{22} (R_{\text{flow}}/0.5 \text{ kpc}) \text{ cm}^{-2}$ before escaping from the flow. Here, R_{flow} denotes the radius associated with the characteristic cross-sectional area of each stream³. Scattering through such large columns broadens the Ly α line to a width of $\sim 800 (N_{\text{HI}}/10^{22} \text{ cm}^{-2})^{1/3} (T_c/10^4 \text{ K})^{1/6} \text{ km s}^{-1}$ (Neufeld 1990). Velocity gradients that exist throughout the flow will reduce this broadening; when velocity gradients are present, the relevant length scale – and hence column

³ The cross-sectional radius of a cold filament can be estimated as follows. The total solid angle that is covered by the cold gas at a distance r from the center of the halo is $\Omega_{\text{cold}}(r) = 4\pi \times (f_{\text{cold}} \frac{T_c}{T_{\text{vir}}})$. Cold accretion typically occurs via multiple cold streams, and the average solid angle that is covered by a single cold filament is $\Omega_{\text{fil}}(r) = \frac{1}{N_{\text{fil}}} \times 4\pi \times (f_{\text{cold}} \frac{T_c}{T_{\text{vir}}})$, where N_{fil} is the total number of filaments. From this it follows that the angular size of a single cold flow in radians, when viewed from the center of the halo, is $\theta_{\text{fil}} = \sqrt{\frac{1}{N_{\text{fil}}} \times 4\pi \times (f_{\text{cold}} \frac{T_c}{T_{\text{vir}}})}$, which translates to a physical radius of $R_{\text{flow}}(r) = \theta_{\text{fil}} r$. Substituting numbers yields $R_{\text{flow}} = 0.8 (N_{\text{fil}}/5)^{-1/2} (r/0.5 r_{\text{vir}}) \text{ kpc}$ (where the mass dependence enters only through f_{cold}).

density – that set the amount of velocity broadening is the Sobolev length, defined as the length over which the velocity changes by one thermal width $l_s \equiv v_{\text{th}}/[dv(r, R)/dR]$ (Bonilha et al. 1979, and see e.g. § 6.2 in Dijkstra & Loeb 2008b). Here, R denotes the transverse direction in the cold flow. If for example, $dv/dR \sim v_{\text{circ}}/R$ (which appears reasonable for some cold filaments based on inspection of Figs. 8 & 9 of Dekel et al 2009), then we get that the total amount of velocity broadening is reduced by a factor of $(v_{\text{circ}}/v_{\text{th}})^{1/3} \sim 2.6 (M_{\text{halo}}/10^{12} M_\odot)^{1/9}$. We therefore conclude that although scattering plays a non-negligible role in broadening the Ly α line profile, it does not lead to Ly α velocity widths that exceed those of the observed blobs. However, the complexity of the associated radiative transfer effects does not allow us to make precise predictions for the Ly α line width and its relation to the halo mass (or corresponding Ly α luminosity).

Because of the low volume filling factor of the cold flows, we do not expect the Ly α photons to scatter off neutral hydrogen (HI) in separate cold filaments once they have escaped from their filament of origin. For this reason, scattering will lead to a very low level of polarization (or none at all) for these models, in difference from the models of Dijkstra & Loeb (2008) who predicted high levels of polarization for Ly α emerging from neutral, spherically symmetric, collapsing gas clouds. In addition, we do not expect the systematic blueshift of the Ly α line that was predicted Dijkstra et al. (2006) for spherically symmetric models⁴.

Some resonant scattering would occur for photons that enter the IGM blueward of the line resonance. The impact of the IGM would be frequency-dependent, and we expect the associated ‘blurring’ to be most prominent for the most energetic Ly α photons. The resonantly scattered Ly α radiation is expected to have a low level ($\lesssim 7\%$) of linear polarization (Dijkstra & Loeb 2008).

The observed LABs have a large spatial extent (Steidel et al. 2000) of $\sim 150 \text{ kpc}$. In our simplified treatment, Ly α is emitted from a region that extends out to the virial radius of the host halo,

$$r_{\text{vir}} \approx 82 \text{ kpc} \left(\frac{M_{\text{halo}}}{10^{12} M_\odot} \right)^{1/3} \left(\frac{1+z}{4} \right)^{-1}. \quad (8)$$

This implies LABs with diameters of ~ 160 –350 kpc for halo masses in the range of $M_{\text{halo}} \sim 10^{12}$ – $10^{13} M_\odot$. This range is expected to exceed the observed blob sizes, since our estimate was derived under the simplifying assumption of a gravitational heating efficiency f_{grav} that is independent of

⁴ Interestingly, Adams et al. (2009) did recently detect a systematic blueshift of the Ly α line relative to the observed 21-cm absorption line. They simultaneously reproduced both observations with radiative transfer of Ly α through a spherically symmetric, neutral collapsing gas cloud with a gas mass of $M_{\text{gas}} \sim 10^{12} M_\odot$. Unless the mass of the host dark matter halo is implausibly high, $M_{\text{halo}} \sim 10^{14} M_\odot$, this would require an unusually high fraction of the gas to be in the cold phase (with f_{cold} close to unity). This inference might imply a significant scatter in f_{cold} for a given halo mass. Some scatter in f_{cold} is indeed observed in simulations, although not at the level to explain cold fractions close to unity. The possible existence of large f_{cold} values would only boost the predicted number of cooling powered blobs and strengthen our basic conclusions.

radius. Higher resolution AMR simulations by Agertz et al. (2009) show that cold streams slow down progressively after they enter the inner halo ($r \lesssim 0.3 - 0.5r_{\text{vir}}$), and therefore suggest that f_{grav} is likely to increase at smaller radii. Models that account for this increase predict smaller blob sizes that are closer to the observed values. It is also possible that existing observations only detect Ly α radiation from the inner regions of cold flows where the Ly α surface brightness is high. Indeed, $\sim 60 - 70\%$ of our computed Ly α luminosity emerges from $r < 0.5r_{\text{vir}}$ (with this modest reduction factor having a negligible effect on Fig. 4). In this case, deeper observations would reveal filamentary extensions of the blobs to larger scales.

4.2 The Role of Dust

Neutral gas in the cold flows forces each Ly α photon to scatter multiple times before escaping from the flow. As a result, Ly α photons traverse on average a total distance through the cold flow that is $\sim 130(N_{\text{HI}}/10^{22} \text{ cm}^{-2})^{1/3}(T_c/10^4 \text{ K})^{1/6}$ times larger than that for continuum photons (Adams 1975). One would therefore expect the Ly α flux to be highly susceptible to absorption by dust. In reality, dust extinction is probably not an important effect since the cold flows consist of compressed intergalactic gas that has not been processed through galaxies. We therefore expect these flows to contain significantly less dust than the interstellar medium of star forming galaxies. Indeed, it is likely that quenching of Ly α flux by dust is more important for superwind-generated emission (see § 4.4 for a discussion of alternative models for Ly α blobs), since in this case the Ly α flux is generated in cold neutral shells of gas that were swept up from the interstellar medium of the galaxy. Mori et al. (2004) found the dust-opacity to Ly α of their superwind generated shells to be negligible ($\tau_d \sim 0.03[N_{\text{HI}}/5 \times 10^{21} \text{ cm}^{-2}]$). However, their estimate of τ_d does not take into account the fact that scattering can boost the total distance traversed by Ly α photons through the shell – and therefore the optical depth – by a factor of $\sim 110(T_c/10^4 \text{ K})^{1/6}$ to a value of $\tau_d \sim 3.3(N_{\text{HI}}/5 \times 10^{21} \text{ cm}^{-2})(T_c/10^4 \text{ K})^{1/6}$. It is therefore a serious concern that the dust opacity to Ly α photons in these models exceeds unity.

On the other hand, the cold flows are expected to contain significantly less dust because they originate in the , and so we conclude that the Ly α flux generated in cold flows is not subject to the same level of dust opacity. For a typical intergalactic gas metallicity $Z \sim 10^{-3}Z_{\odot}$ (e.g. Schaye et al. 2003), and for typical HI column densities and velocity gradients in the cold flows (see § 4.1), we expect a dust opacity that is well below unity. This low level of enrichment is not unreasonable, as galactic outflows would typically avoid the overdense inflowing filaments. Indeed, preliminary simulations indicate that outflows generally enrich the large volume surrounding the voids, while leaving the cold flows metal poor (R. Joung, private communication).

4.3 The ‘Duty Cycle’ of the Cold Accretion Mode

When computing the cumulative luminosity function of blobs through Eq. (2), we implicitly assumed a duty cycle of unity. That is, we assumed each massive galaxy halo

to be surrounded by cold flows. Simulations support this assumption: the massive halos which produce a detectable Ly α luminosity typically reside in overdense regions of the Universe in which accretion of cold gas from filaments onto the more massive halos is a continuous process at redshifts $z \gtrsim 2$. This is in sharp contrast to intense starburst and/or quasar activity, which occur with duty cycles that are much smaller than unity. Indeed, in our model the cold flows are luminous in Ly α irrespective of the activity in the central galaxy, which explains why only a fraction of Ly α blobs are observed to be associated with intense starburst or quasar activities.

4.4 Comparison to Other ‘Blob Models’

While the cold accretion model can successfully reproduce the abundance of LABs in the Universe as well as their physical properties, it is useful to compare our model to the other models for LABs mentioned in § 1. The observed number density of blobs, combined with their preferred residence in dense regions of our Universe, requires an association with massive halos ($M_{\text{halo}} \sim 10^{12} - 10^{13} M_{\odot}$).

An association with bright quasars also naturally places the blobs in massive halos (Hopkins et al. 2007). However, the filamentary geometry of the simulated cold gas shield it from any central source of ionizing radiation, suppressing the photoionization rate by the quasar. Furthermore, the short duty cycle of quasar activity (Martini 2004) is problematic. Indeed, a large fraction of blobs have no associated quasar nearby (see Bunker et al. 2003; Weidinger et al. 2004, for examples of Ly α blobs associated with radio quiet type I Active Galactic Nuclei (AGN)).

The duty cycle argument, combined with the lack of the relevant associated sources, argues against photoionization by inverse Compton radiation, or star formation that is triggered by AGN jets. Formally, photoionization by regular star forming galaxies (LBGs) is not ruled out for $\sim 60\%$ of Ly α blobs (e.g. Matsuda et al. 2004). However, it remains to be explained why the LBGs in these dense environments would be so efficient at generating Ly α radiation, while observationally it is known that the escape fraction of Ly α radiation from LBGs is typically low, and that only 20 – 25% of $z = 3$ LBGs would even classify as a Ly α emitting galaxy (Shapley et al. 2003). Indeed, for this reason Jimenez & Haiman (2006) argued for photoionization by primordial galaxies which can emit more ionizing photons per observed rest-frame UV continuum. This is an interesting suggestion, although it remains to be shown that the gas in highly overdense, evolved, regions of our Universe can remain pristine down to $z = 3$ at a level that is needed to explain the Ly α blobs.

In any case, all photoionization models require cold spatially extended gas to be present in these halos, because the gas at the virial temperature of these halos ($T_{\text{vir}} \gtrsim 2 \times 10^6 \text{ K}$) would recombine too slowly to reproduce the observed Ly α luminosities. Indeed, Haiman & Rees (2001) obtain their Ly α recombination radiation – following photoionization by the central quasar – from cold ($T = 10^4 \text{ K}$) gas clouds embedded in a hot medium, very similar to the cold-accretion scenario that is seen in galaxy-formation simulations (the main difference being that the cold phase consists of separate clouds in the early models [such as in Fall & Rees 1985]

rather than long continuous streams). Because photoionization models require the existence of cold spatially extended gas, they may be viewed as a special case of the cold accretion model in which the heating rate $H(r)$ is dominated by photoheating (although it remains to be shown that the gas does not self-shield). In principle the photoionization models also work when the cold gas is supplied by outflowing material (see below). However, dust in outflow models is a bigger problem here than for the inflow models (see § 4.2).

A fundamentally different model for blobs is the superwind model. The association of some blobs with submm sources imply a connection with starburst galaxies (having star formation rates of $\sim 10^{2-3} M_{\odot} \text{ yr}^{-1}$). The kinetic energy associated with the starburst-driven superwinds is sufficient to power the Ly α emission in LABs (Taniguchi & Shioya 2000; Geach et al. 2005). However, it is not clear that this coupling of energy occurs naturally at the level that is required to explain the LABs. Mori et al. (2004) used hydrodynamical simulations to show that superwinds driven by a starburst ($\dot{M}_{*,\text{max}} \sim 200 M_{\odot} \text{ yr}^{-1}$) can produce an LAB that closely resembles one of Steidel et al. (2000) blobs in appearance, but with a luminosity that is $\sim 10/\mathcal{T}_{\alpha}$ times too small (note that $\mathcal{T}_{\alpha} < 1$). If we simply scale up the luminosity of an LAB in proportion to the total star formation rate, then the observed Ly α luminosity requires a star formation rate of $\sim 2000/\mathcal{T}_{\alpha} M_{\odot} \text{ yr}^{-1}$. However, this is close to the observed star formation rate derived from the detected sub-millimeter flux in only one of Steidel et al.'s LABs (Geach et al. 2005). Also, the conversion from star formation rate to the blob's Ly α luminosity assumed that the dust opacity for Ly α photons is negligible. We showed in § 4.2 that this may not be correct when radiative transfer effects are accounted for. Furthermore, not all blobs have starburst activity associated with them (Matsuda et al. 2006; Nilsson et al. 2006; Smith & Jarvis 2007; Saito et al. 2008; Smith et al. 2009), thus ruling out this model for these sources.

4.5 Testable Predictions of the Cold Accretion Model For Ly α Blobs

Simulations suggests that the cold flows enter the center of the halo as multiple filamentary streams. This filamentary structure is expected to show up in the observations. In § 4.1 we argued that some 'blurring' of the Ly α image may be expected, but only for the most energetic Ly α photons, as these are expected to resonantly scatter in the IGM. Existing images of LABs typically have an angular resolution of ~ 1 arcsec, which corresponds to ~ 8 kpc at $z = 3$. Therefore, existing observations would not resolve the filaments yet, although the filamentary nature of the cold flows may show up at larger radii (where different filaments are well-separated). Existing observations of blobs that are presently thought to be powered by cold accretion do show some interesting irregularities in their images (Nilsson et al. 2006; Smith et al. 2008a), but the quality of the data does not allow to classify the image as 'filamentary'. It is intriguing that the images of some of the LABs discovered by Matsuda et al. (2004) are very irregular, and possibly filamentary (e.g. blob 6, 9, 11, and 12). If these blobs are associated with cold flows, then we expect deeper and higher resolution images of the blobs to more clearly reveal the filamentary structure.

We argued in § 4.1 that we do not expect the systematic blueshift of the Ly α line, nor the high level of polarization, that were predicted by spherically symmetric models of neutral collapsing gas cloud. This is mostly because the Ly α photons scatter mostly in the filament where they were produced, after which they escape to the observer (following some resonant scattering in the IGM). Because the fraction of cold accreting gas increases towards lower galaxy masses (and therefore lower blob luminosities in our model), we may expect cold accretion to be less filamentary at lower galaxy masses. This implies that the predictions of the models that assumed spherically symmetric accretion – involving the blueshift and the high levels of linear polarization – may be increasingly relevant at lower halo masses and blob luminosities. However, these trends are rather weak in the limited range of halo masses of interest here, $M_{\text{halo}} = 10^{12} - 10^{13} M_{\odot}$ (see e.g. Fig 5 and Fig 6 of Keres et al. 2009, but see Adams et al. 2009 and § 4.1).

In our model, the vast majority of the Ly α radiation is generated from collisional excitation of atomic hydrogen. At temperatures of $T_c \sim 10^4$ K, collisional excitation of the Ly β transition is ~ 10 times less effective. Therefore, we expect an H α ($\lambda = 6536 \text{ \AA}$) flux that is $\sim 10\mathcal{T}_{\alpha} \times 6536/1216 \sim 54\mathcal{T}_{\alpha}$ times lower. This is unfortunate because a combined measurement of the Ly α and H α fluxes could have constrained the importance of radiative transfer effects. In § 4.1 we concluded that radiative transfer effects were not negligible, and that they may noticeably broaden the Ly α line. To find this broadening requires the detection of the much fainter H α line. It is not guaranteed that the H α flux will actually be suppressed by a factor as large as that mentioned above. As we argued in § 4.6, the weak shocks that heat the cold flows on their way to the halo center, may occasionally heat the gas to a temperature at which hydrogen becomes significantly ionized. In this case, the H α flux may be down by the value expected from recombinations ($\sim 9\mathcal{T}_{\alpha}$). These shocks may also result in helium becoming singly ionized, leading to a detectable He 1640 emission (Yang et al. 2006).

The observed LAB luminosity function (which we compiled from the data presented by Matsuda et al. (2004)) is reproduced by models in which $\mathcal{T}_{\alpha} f_{\text{grav}} \sim 0.15$ (for $\delta_M(V_s) = 3\sigma_M(V_s)$, see Fig. 1). Assuming that $\mathcal{T}_{\alpha} f_{\text{grav}} \sim 0.15$ (independent of redshift), we can predict Ly α luminosity functions for accretion powered LABs at $z = 2$ and $z = 4$ (when averaged over large regions of our Universe, such that $\delta_M(V_s) \sim 0$). These luminosity functions are shown in Figure 5, which implies that a decline in the number density of accretion powered blobs more luminous than a few $\times 10^{43} \text{ erg s}^{-1}$ is expected beyond $z = 3$. Such a decline – if present – could be detected with future observations. For example, the *Hobby-Eberly Telescope Dark Energy Experiment* (HETDEX, Hill et al. 2008) is expected to detect 0.8 million Ly α emitting galaxies and therefore thousands of LABs at $1.9 < z < 3.5$. Such a large sample of blobs will allow for accurate measurements of their spatial clustering, and luminosity functions. The combination of these measurements should place tight constraints on blob formation models.

4.6 Discussion of Model Uncertainties

We have taken the total fraction of the gas that is in cold streams as a function of halo mass from the most recent

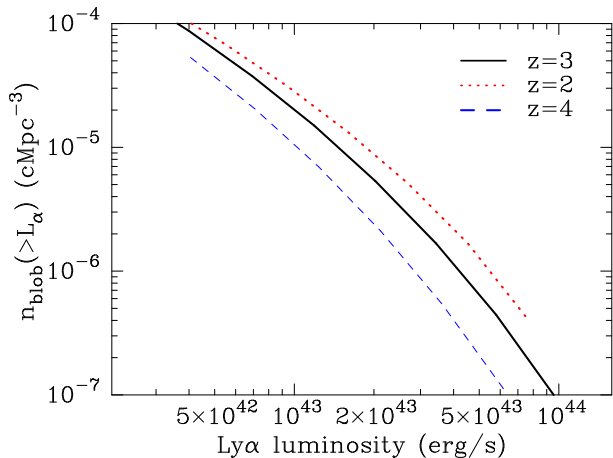


Figure 5. The predicted cumulative luminosity functions of cold-accretion powered LABs at $z = 2$ (red dotted line), $z = 3$ (solid line), and $z = 4$ (blue-dashed line) (in a region at mean cosmic density) for $f_{\text{grav}}\mathcal{T}_\alpha = 0.15$ (the value preferred by fitting to the data of Matsuda et al 2004; see text). A drop in the number density of sources more luminous than a few $\times 10^{43}$ erg s^{-1} is expected beyond $z = 3$. This drop may be enhanced by the that becomes increasingly opaque with increasing redshift.

simulations of cold streams in massive halos (see § 1). Other model assumptions that were described in § 2 were based on these same simulations. However, the cold flow properties in our model - in particular the gas density and temperature - can be quite different from what is seen in the simulations. These differences are mostly due to the simplified nature of our model which assumes a two-temperature baryonic component, while in reality there is a wider spread in temperatures in the cold streams (a more detailed discussion follows below). We have not attempted to bring our model in closer agreement to the simulations because it would require more detailed modeling of increasingly uncertain physical processes. Most importantly, we will show below that these differences are not important as far the Ly α emissivity of the cold gas is concerned. In the following we address the differences in cold flow properties between our model and the simulations, and discuss other model uncertainties in more detail.

4.6.1 Our Model versus Simulations: Cold Flow Temperature and Density

Our models predict gas densities that are significantly higher than those observed in AMR simulations (e.g. Dekel et al. 2009). For a $M_{\text{halo}} = 10^{12} M_\odot$ halo, we find $n_c \sim 1 \text{ cm}^{-2}$ at $r = 0.3r_{\text{vir}}$, which is about a factor of ~ 30 larger than the mean cold flow density that is found in the simulations. Similarly, the hot gas in our model denser by about a factor of $\sim 3 - 4$ (A. Dekel, private communication). There are several reasons for this discrepancy: (i) the simulated flows are at a somewhat lower redshift ($z = 2.5$) than we consider ($z \sim 3$), which reduces the density by a factor of $(4/3.5)^3 \sim 1.5$; (ii) the cold fraction of gas is slightly higher in AMR simulations ($f_{\text{cold,AMR}} = 0.4-0.5$ at $M_{\text{halo}} = 10^{12} M_\odot$, see Birnboim et al. 2007) than in the SPH simulations, which reduces the number density of particles in the hot phase. This amounts to an additional factor of $(1 - f_{\text{cold,SPH}})/(1 -$

$f_{\text{cold,AMR}}) \sim 1.5$. When combined, this explains a factor of $(1.5)^2 = 2.25$. The remaining difference in the hot gas density is at the factor $\lesssim 2$ level, which may be due to the details of gas density profile that was used (also see § 4.6.2).

The fact that the density discrepancy is stronger for the cold gas suggests that pressure equilibrium is not exactly satisfied in the simulation. Indeed, in AMR simulations $P_{\text{cold}} \sim 0.5P_{\text{hot}}$ at $r \lesssim 0.5r_{\text{vir}}$ (A. Dekel, private communication) which implies that at a given temperature, the number density in the simulated cold gas is reduced by an extra factor of ~ 2 . Furthermore, the gas temperatures in the simulated cold gas are somewhat higher (a more detailed discussion of this follows below) which can lower the density by an extra factor of ~ 2 . When collecting all factors of 2 and 1.5, an order of magnitude difference in gas density can be accounted for. The remaining difference in the cold gas density is at the factor ~ 3 level, which may again be due to the details of gas density profile that was used (also see § 4.6.2).

We emphasize that because of our requirement that the cooling rate balances the local heating rate, $H(r)$, our predicted Ly α luminosity is not affected by the exact density in the cold gas at all. This is because the heating rate (Eq 1) is independent of gas density and temperature. Furthermore, radiative cooling is dominated by the emission of Ly α photons at the typical cold gas temperatures. We therefore indirectly regulate the Ly α emission rate *per hydrogen atom* by the local heating term. When the cold flow gas density is lowered/raised, a fixed cooling rate is maintained by raising/lowering the cold gas temperature. For a fixed cold gas mass, we therefore predict a fixed Ly α luminosity that depends almost entirely on the heating rate. Formally, there is a (very) weak temperature -and hence density- dependence of what fraction of the total cooling (and therefore heating) rate emerges as Ly α line photons. For example, at the temperatures that we encounter in our model $\sim 63 - 67\%$ of the all cooling radiation is in Ly α line photons, while at $T=2 \times 10^4$ K this fraction reduces to $\sim 50\%$. The resulting very weak density dependence of the predicted Ly α luminosity has no impact on our results.

In our model, the halo gas consists of 'hot' and 'cold' components. The hot gas is at virial temperature of the halo, $T_{\text{vir}} = 1.9 \times 10^6 \text{ K} (M_{\text{halo}}/10^{12} M_\odot)^{2/3} [(1+z)/4]$, while the cold flows have a typical temperature of $T_c \sim 0.95-1.2 \times 10^4$ K due to efficient cooling (as the atomic cooling rate of the gas is high above 10^4 K and drops sharply below this value). Simulations show a wider spread in temperatures of the cold gas, namely $T_c \sim 10^4-10^5$ K. This apparent discrepancy is not serious, as the gas at 10^5 K (in the SPH simulations) is mostly concentrated near the outermost regions of the halo where cooling is less efficient. The vast majority of the gas in the inner regions is in the range $T \sim 1 - 2 \times 10^4$ K. Furthermore, the SPH simulations do not take into account self-shielding of the gas (D. Keres, private communication), which implies that photoheating is boosted artificially. More importantly, ignoring self-shielding artificially suppresses the efficiency with which the gas can cool (e.g. see Fig 2 of Katz et al. 1996). This at least partially explains the somewhat higher temperatures observed in these simulations.

Lastly, the processes that are responsible for heating the cold flows may occasionally heat the gas to higher tem-

peratures, $T \sim 2 \times 10^4 - 10^5$ K, after which it would rapidly cool to lower temperatures. The warmest regions could be bright in emission of the He 1640 Å line (Yang et al. 2006), but at levels that are at most $\sim 1-2$ orders of magnitude lower than the total flux in the HI Ly α line (which is barely affected by these rare warmer regions inside the cold flow). Hydrogen is mostly ionized at $T \sim 2 \times 10^4$ K, which results in recombination radiation. This would boost the expected H α flux emitted by the cold flows relative to the H α -flux expected from purely collisionally excited HI (see § 4.5).

An important caveat to the simulations of cold flows is that they do not incorporate superwinds that are generated by star-forming regions. Superwinds can drive large-scale outflows that act as a source of Ly α emission (Mori et al. 2004). These winds expand most efficiently into the lower density regions and will probably not affect the cold flows because of the small solid angle occupied by the cold filaments. Indeed, preliminary analysis of simulations that do take into account winds support this claim (D. Keres, private communication). Therefore, winds are expected to provide an additional source of Ly α radiation, but would not disrupt the formation of Ly α photons by gravitational heating of cold streams. Below we show that this additional 'wind-generated' Ly α flux is likely comparable or less than the flux from the cold flows.

4.6.2 Energy Dissipation in the Hot Gas and Dynamical Instabilities in the Cold Flows

We assumed that no energy was dissipated in the hot gas, i.e. $f_{\text{hot}} = 0$ in Eq 2. This assumption was motivated by the simulations in which the majority of the cold gas mass is in diffuse continuous streams. This implies that the majority of cold gas is surrounded by other cold gas, and that therefore little interaction occurs between the hot and the majority of the cold gas. However, shearing motions at the interface of the cold and hot gas may trigger the formation of instabilities that are not captured by existing simulations of cold flows. In particular, Kelvin-Helmholtz instabilities that develop at the cold-hot gas interface could completely disrupt the cold stream⁵, but this requires the relative velocity of the cold and hot gas to be subsonic in both frames (e.g. Miles 1957; Bassett & Woodward 1995, and references therein). Because the sound speed in the cold gas is $c_{s,\text{cold}} \sim 13$ km s⁻¹, this requirement is clearly not met. However, the formation of instabilities in cold streams is clearly an issue that needs to be addressed in future work. Instead of disrupting the cold streams, these instabilities can introduce non-negligible amounts of energy dissipation in the hot gas⁶.

We investigate the effect of energy dissipation in the hot gas in Figure 6. Here, we plot Ly α luminosity as a function of halo mass for a model a model in which $f_{\text{hot}} = 0.7$, i.e. $\sim 70\%$ of the gravitational work done on an H-atom goes into heating the hot gas, instead of going into bulk infall motion of the atom (Eq 2). Furthermore, for completeness

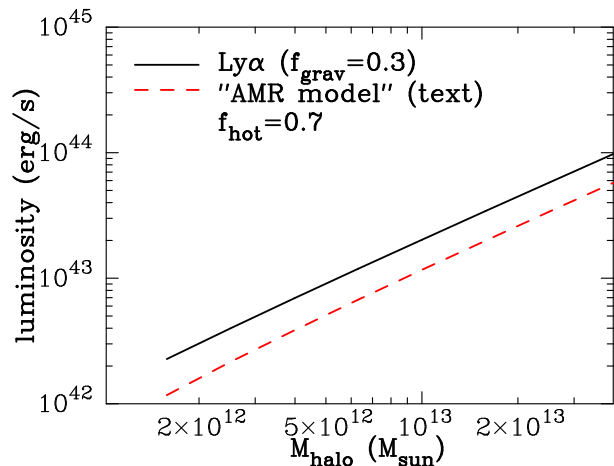


Figure 6. The same as Fig 3. Here, the *red dashed line* represent a model in which a significant fraction of the binding energy is dissipated in the hot gas, $f_{\text{hot}} = 0.7$. Furthermore, we modified densities in the hot and cold gas to more closely resemble those seen in AMR simulations (see text). The overall predicted Ly α luminosities are reduced by a factor of ~ 2 . This can be compensated for by increasing f_{grav} to $f_{\text{grav}} = 0.5$.

we adjust the cold flow properties to more closely resemble those encountered in AMR simulations. In this 'AMR model' we (i) assume different hot gas density and temperature profiles as described in § 2.1 of Dekel & Birnboim (2008, their model with $\alpha_g = 0$), which appear to provide a better description of the hot gas component in the AMR simulation, (ii) reduce the overall gas density by reducing the total gas mass fraction to $f_{\text{gas}} = 0.05$, (iii) boost the overall fraction of the gas in the cold phase by a factor of 2, (iv) assume that $P_{\text{cold}} = 0.5P_{\text{hot}}$. Modifications (ii-iv) reduce the gas density in both the cold and hot phase, and slightly increase the gas temperature in the cold gas (but not to the values that are encountered in the simulations, see § 4.6.1). The overall reduction in the amount of gas by a factor of $\sim 0.08/0.05 = \sim 1.6$ is compensated for by the boost in the cold fraction. However, the reduced infall velocity reduces the local heating rate and thus the overall Ly α luminosity for a given halo. In order to restore the original halo mass-Ly α luminosity relation, we require that $f_{\text{grav}} = 0.5$. Note that it is possible that $f_{\text{grav}} + f_{\text{hot}} > 1$, and it corresponds to a model in which the cold gas decelerates as it descends down the gravitational potential well. In order for solutions to exist for $v(r)$ at all radii, we require that $f_{\text{grav}} + f_{\text{hot}} \lesssim 1.35$. Therefore a significant of the gravitational binding energy may be dissipated in the hot gas without invalidating our model, and for the example discussed above $f_{\text{hot}} \lesssim 0.85$ is tolerated.

4.7 Comparison to Previous Work

The high density gas in the cold flows can cool very efficiently, and without any heat source this gas would almost instantly cool down to temperatures at which the Ly α emissivity would be practically zero. Because the gas densities in the cold flows are high, this gas is capable of self-shielding and photoheating is negligible. We therefore resorted to 'gravitational heating', which refers to the hydro-

⁵ <http://mngrid.ucsd.edu/~akritsuk/renzo/kelvin/kelvin.html>

⁶ Interestingly, these same instabilities would heat the cold gas through weak shocks, thus providing another physical mechanism by which gravitational binding energy is converted into heat in the cold gas.

dynamical heating that the cold gas undergoes as it navigates down to the center of the dark matter potential. This gravitational heating mechanism was described in an analytic model by Haiman et al. (2000) who predicted the existence of Ly α blobs as a result of this cooling radiation. Fardal et al. (2001) obtained similar results using hydrodynamical simulations -which already contained cold streams of gas, albeit at significantly lower resolution. In both papers, the gas emitted all its gravitational binding energy as cooling radiation prior to reaching the central galaxy. This scenario would translate to $f_{\text{grav}} \geq 1$ in our model. Our work may be viewed as an important improvement over - or an extension of - previous work, because our model is likely immune to various important objections that can be raised against older models: (i) we have shown that a significant of the gravitational binding energy may be dissipated in the hot gas without invalidating our conclusions (§ 4.6.2), (ii) in our model, gas accretion occurs along dense, compressed, flows that cover a tiny solid angle when viewed from the center of their host halo. Therefore, these cold flows could not be easily disrupted by powerful outflows from starburst activity or AGN, which would preferentially propagate into the lower density (volume filling) phase of the halo gas. This implies that cold flows can coexist with powerful sources, as observed for some of the LABs (Chapman et al. 2001; Basu-Zych & Scharf 2004; Geach et al. 2007, 2009). For the same reason, we do expect these outflows to enrich the inflowing cold streams with metals and dust, which could severely quench the Ly α flux from the cold streams (see § 4.2).

More recently, Furlanetto et al. (2005) used high resolution SPH simulations to study Ly α emission from structure formation, which included cold flows. In their highest resolution simulations, Furlanetto et al. (2005) have a spatial resolution of ~ 1 kpc which is comparable to that of Kereš et al. (2009), but in a cosmological volume that is too small to contain the massive halos that we associate with Ly α blobs. Despite the absence of these massive halos, these simulations contained luminous blobs with properties that resemble the observed ones. Hence, these models -just like the models of Haiman et al. (2000) and Fardal et al. (2001)-overproduce the number density of blobs: existing observations suggest that the field SSA21 contains a number density of blobs that is ~ 10 – 10^2 larger than the Universe as a whole (see § 3.2 and Fig 4). Ly α blobs are likely rarer than was originally thought.

Simulations thus seemed to create luminous Ly α blobs ($L_{\text{Ly}\alpha} \sim 10^{44}$ erg s $^{-1}$) around too abundant lower mass halos. This may partly be due to the fact that simulations contain a non-negligible fraction of cold gas that is locked up into denser clumps which reside both inside and outside the cold flows. Because of their enhanced density, most of the Ly α luminosity would come from these discrete clumps. These clumps may also be sites in which stars form which may boost the Ly α emissivity from these clumped regions even more. However, it is likely that Ly α emission does not escape efficiently from star forming regions at $z = 3$: observations of $z = 3$ Lyman break galaxies (LBGs) suggest that ~ 20 – 25% of star forming galaxies has a strong enough observed Ly α emission line to classify as a Ly α emitting galaxy (Shapley et al. 2003). Furthermore, a significant fraction of these Ly α emitting galaxies have emission lines that

are weaker than expected on the basis of recombination theory (Dijkstra & Westra 2009). Without a good model for how Ly α escapes from these clumps, their Ly α luminosity may well have been overestimated. This could explain why simulations have overpredicted the number density of Ly α emitting blobs. Alternatively, the simulated cold flows are too warm (see e.g. Furlanetto et al. 2005, for a discussion on why gas temperatures in self-shielded regions are notoriously difficult to simulate). As was mentioned earlier (§ 4.6.2), the gas temperature in our 'AMR model' was below that encountered in the simulation. This suggests that the AMR simulation also associates (much) more luminous Ly α blobs to halos of a given halo mass than our model. This may result in a predicted number density of Ly α blobs that is at odds with the observations.

5 CONCLUSIONS

Recent hydrodynamical simulations of the formation of galaxies show that baryons assemble into galaxies through a two-phase medium which contains filamentary streams of cold ($T \sim 10^4$ K) gas in pressure equilibrium with a hot gaseous halo (e.g Kereš et al. 2005; Ocvirk et al. 2008; Dekel et al. 2009; Kereš et al. 2009; Agertz et al. 2009). These cold flows contain ~ 5 – 25% of the total gas content (Kereš et al. 2009) in halos as massive as $M_{\text{halo}} \sim$ a few $10^{13} M_{\odot}$ (Dekel et al. 2009).

At the typical densities and scales of the cold flows ($n_c \gtrsim 1$ cm $^{-3}$), the gas is self-shielded from external ionizing radiation (see § 3.1) and is heated through gravitational contraction. We have demonstrated that if $\gtrsim 10\%$ of the change in the gravitational binding energy of a cold flow goes into heating of the gas, then the simulated cold flows are spatially extended Ly α sources with luminosities and number densities that are comparable to those of observed Ly α blobs (see Fig 4).

Furthermore, the typical velocity widths of the LABs span the range (Matsuda et al. 2006) of 500–1700 km s $^{-1}$, which is consistent with the model in which infall occurs at velocities in the range 1.0 – $2.5v_{\text{circ}} \sim 220$ – 1500 km s $^{-1}$, which naturally result in the observed velocity widths (see § 4.1). The filamentary structure of the cold flows may explain the wide range of observed Ly α blob morphologies.

The association with massive halos naturally places LABs in overdense regions (Steidel et al. 2000; Matsuda et al. 2004, 2006). Furthermore, the simulated cold flows are dense and cover only a small solid angle when viewed from the center of their host halo. Therefore, they could not be easily disrupted by powerful outflows from starburst activity or AGN, which would preferentially propagate into the lower density (volume filling) phase of the halo gas. This implies that cold flows can coexist with powerful sources, as observed for some of the LABs (Chapman et al. 2001; Basu-Zych & Scharf 2004; Geach et al. 2007, 2009). The association of LABs with sub-mm sources or AGN is not surprising, since these sources are triggered by the infall of cold gas into massive galaxies. Even when the central sources are sufficiently energetic to power the observed Ly α emission, this causal relationship may be difficult to achieve (see § 4.4). Our model associates the spatially extended Ly α emission

with the independent process of cooling within the dense streams of inflowing cold gas. This resolves the puzzling observation that very similar LABs may have completely different sources associated with them (Geach et al. 2007; Yang et al. 2009).

Of course, it is possible that cold flows are partially photoionized by an associated hard X-ray source (as is observed for $\sim 17\%$ of the blobs Geach et al. 2009), or by star forming galaxies that are embedded within the cold flow (Furlanetto et al. 2005). In these cases, the heating rate would be (locally) boosted. This would only make our total predicted Ly α luminosities from the cold flows larger, and would strengthen our conclusion that Ly α blobs are an observational signature of cold accretion into galaxies.

Regardless of the precise heating mechanism, the cold flows should reveal their filamentary geometry in deeper and or higher resolution images (see § 4.5). Once this gas geometry has been probed, it may be possible to constrain the dominant heating mechanisms of the cold gas as it navigates toward the center of the dark matter halo potential. Alternatively, if one does not find any evidence for filamentary spatially extended Ly α sources in the near future, then this is equally interesting, because this may suggest that the simulated cold flows are different than the flows that occur in nature, or - worse - do not represent reality at all (see § 4.6.2 for a discussion on instabilities that may affect cold flow properties). In either case, Ly α observations are expected to provide us with unique constraints on this intriguing mode of gas accretion onto galaxies.

Acknowledgments This work is supported by Harvard University funds. We thank Dušan Kereš, Yuval Birnboim, Zoltán Haiman, Ryan Joung, Renyue Cen, Avishai Dekel, Claude-André Faucher-Giguère, Matt McQuinn and Adam Lidz for useful discussions.

REFERENCES

- Adams, T. F. 1975, *ApJ*, 201, 350
 Adams, J. J., Hill, G. J., & MacQueen, P. J. 2009, *ApJ*, 694, 314
 Adelberger, K. L., Steidel, C. C., Pettini, M., Shapley, A. E., Reddy, N. A., & Erb, D. K. 2005, *ApJ*, 619, 697
 Agertz, O., Teyssier, R., & Moore, B. 2009, *MNRAS*, 397, L64
 Barkana, R., & Loeb, A. 2001, *PhR*, 349, 125
 Barkana, R., & Loeb, A. 2004, *ApJ*, 609, 474
 Bassett, G. M., & Woodward, P. R. 1995, *Journal of Fluid Mechanics*, 284, 323
 Basu-Zych, A., & Scharf, C. 2004, *ApJL*, 615, L85
 Birnboim, Y., & Dekel, A. 2003, *MNRAS*, 345, 349
 Birnboim, Y., Dekel, A., & Neistein, E. 2007, *MNRAS*, 380, 339
 Bond, J. R., Cole, S., Efstathiou, G., & Kaiser, N. 1991, *ApJ*, 379, 440
 Bonilha, J. R. M., Ferch, R., Salpeter, E. E., Slater, G., & Noerdlinger, P. D. 1979, *ApJ*, 233, 649
 Bunker, A., Smith, J., Spinrad, H., Stern, D., & Warren, S. 2003, *APSS*, 284, 357
 Chapman, S. C., Lewis, G. F., Scott, D., Richards, E., Borys, C., Steidel, C. C., Adelberger, K. L., & Shapley, A. E. 2001, *ApJL*, 548, L17
 Chapman, S. C., Scott, D., Windhorst, R. A., Frayer, D. T., Borys, C., Lewis, G. F., & Ivison, R. J. 2004, *ApJ*, 606, 85
 Dekel, A., & Birnboim, Y. 2006, *MNRAS*, 368, 2
 Dekel, A., & Birnboim, Y. 2008, *MNRAS*, 383, 119
 Dekel, A., et al. 2009, *Nature*, 457, 451
 Dey, A., et al. 2005, *ApJ*, 629, 654
 Dijkstra, M., Haiman, Z., & Spaans, M. 2006, *ApJ*, 649, 14
 Dijkstra, M., Lidz, A., & Wyithe, J. S. B. 2007, *MNRAS*, 377, 1175
 Dijkstra, M., & Loeb, A. 2008, *MNRAS*, 386, 492
 Dijkstra, M. 2009, *ApJ*, 690, 82
 Dijkstra, M., Westra, E., *MNRAS* in press
 Fall, S. M., & Rees, M. J. 1985, *ApJ*, 298, 18
 Fardal, M. A., Katz, N., Gardner, J. P., Hernquist, L., Weinberg, D. H., & Davé, R. 2001, *ApJ*, 562, 605
 Faucher-Giguère, C.-A., Lidz, A., Hernquist, L., & Zaldarriaga, M. 2008a, *ApJL*, 682, L9
 Faucher-Giguère, C.-A., Prochaska, J. X., Lidz, A., Hernquist, L., & Zaldarriaga, M. 2008b, *ApJ*, 681, 831
 Furlanetto, S. R., Schaye, J., Springel, V., & Hernquist, L. 2005, *ApJ*, 622, 7
 Geach, J. E., et al. 2005, *MNRAS*, 363, 1398
 Geach, J. E., Smail, I., Chapman, S. C., Alexander, D. M., Blain, A. W., Stott, J. P., & Ivison, R. J. 2007, *ApJL*, 655, L9
 Geach, J. E., et al. 2009, *ApJ*, 700, 1
 Gao, L., Navarro, J. F., Cole, S., Frenk, C. S., White, S. D. M., Springel, V., Jenkins, A., & Neto, A. F. 2008, *MNRAS*, 387, 536
 Giodini, S., et al. 2009, arXiv:0904.0448
 Haiman, Z., Spaans, M., & Quataert, E. 2000, *ApJL*, 537, L5
 Haiman, Z., & Rees, M. J. 2001, *ApJ*, 556, 87
 Harrington, J. P. 1973, *MNRAS*, 162, 43
 Hill, G. J., et al. 2008, *Astronomical Society of the Pacific Conference Series*, 399, 115
 Hopkins, P. F., Lidz, A., Hernquist, L., Coil, A. L., Myers, A. D., Cox, T. J., & Spergel, D. N. 2007, *ApJ*, 662, 110
 Hui, L., & Gnedin, N. Y. 1997, *MNRAS*, 292, 27
 Izotov, Y. I., Thuan, T. X., & Lipovetsky, V. A. 1997, *ApJS*, 108, 1
 Jimenez, R., & Haiman, Z. 2006, *Nature*, 440, 501
 Katz, N., & Gunn, J. E. 1991, *ApJ*, 377, 365
 Katz, N., Weinberg, D. H., & Hernquist, L. 1996, *ApJS*, 105, 19
 Keel, W. C., Cohen, S. H., Windhorst, R. A., & Waddington, I. 1999, *AJ*, 118, 2547
 Kereš, D., Katz, N., Weinberg, D. H., & Davé, R. 2005, *MNRAS*, 363, 2
 Kereš, D., Katz, N., Fardal, M., Davé, R., & Weinberg, D. H. 2009, *MNRAS*, 395, 160
 Komatsu, E., et al. 2009, *ApJS*, 180, 330
 Lidz, A., McQuinn, M., Zaldarriaga, M., Hernquist, L., & Dutta, S. 2007, *ApJ*, 670, 39
 Madau, P. 1995, *ApJ*, 441, 18
 Makino, N., Sasaki, S., & Suto, Y. 1998, *ApJ*, 497, 555
 Martini, P. 2004, *Coevolution of Black Holes and Galaxies*, 169
 Matsuda, Y., et al. 2004, *AJ*, 128, 569
 Matsuda, Y., et al. 2005, *ApJL*, 634, L125

Matsuda, Y., Yamada, T., Hayashino, T., Yamauchi, R., & Nakamura, Y. 2006, *ApJL*, 640, L123

Matsuda, Y., Iono, D., Ohta, K., Yamada, T., Kawabe, R., Hayashino, T., Peck, A. B., & Petitpas, G. R. 2007, *ApJ*, 667, 667

Miles, J. W. 1957, *Acoustical Society of America Journal*, 29, 226

Mori, M., Umemura, M., & Ferrara, A. 2004, *ApJL*, 613, L97

Neufeld, D. A. 1990, *ApJ*, 350, 216

Nilsson, K. K., Fynbo, J. P. U., Møller, P., Sommer-Larsen, J., & Ledoux, C. 2006, *A&A*, 452, L23

Navarro, J. F., Frenk, C. S., & White, S. D. M. 1997, *ApJ*, 490, 493

Ocvirk, P., Pichon, C., & Teyssier, R. 2008, *MNRAS*, 390, 1326

Osterbrock, D. E. 1989, *Research supported by the University of California, John Simon Guggenheim Memorial Foundation, University of Minnesota, et al. Mill Valley, CA, University Science Books*, 1989, 422 p.,

Press, W. H., & Schechter, P. 1974, *ApJ*, 187, 425

Rees, M. J., & Ostriker, J. P. 1977, *MNRAS*, 179, 541

Rees, M. J. 1989, *MNRAS*, 239, 1P

Rybicki, G. B., & Lightman, A. P. 1979, *New York, Wiley-Interscience*, 1979. 393 p.,

Scharf, C., Smail, I., Ivison, R., Bower, R., van Breugel, W., & Reuland, M. 2003, *ApJ*, 596, 105

Shapley, A. E., Steidel, C. C., Pettini, M., & Adelberger, K. L. 2003, *ApJ*, 588, 65

Smith, D. J. B., & Jarvis, M. J. 2007, *MNRAS*, 378, L49

Saito, T., Shimasaku, K., Okamura, S., Ouchi, M., Akiyama, M., & Yoshida, M. 2006, *ApJ*, 648, 54

Saito, T., Shimasaku, K., Okamura, S., Ouchi, M., Akiyama, M., Yoshida, M., & Ueda, Y. 2008, *ApJ*, 675, 1076

Schaye, J., Aguirre, A., Kim, T.-S., Theuns, T., Rauch, M., & Sargent, W. L. W. 2003, *ApJ*, 596, 768

Shapley, A. E., Steidel, C. C., Pettini, M., & Adelberger, K. L. 2003, *ApJ*, 588, 65

Sheth, R. K., & Tormen, G. 1999, *MNRAS*, 308, 119

Sheth, R. K., Mo, H. J., & Tormen, G. 2001, *MNRAS*, 323, 1

Shull, J. M., & van Steenberg, M. E. 1985, *ApJ*, 298, 268

Smith, D. J. B., & Jarvis, M. J. 2007, *MNRAS*, 378, L49

Smith, D. J. B., Jarvis, M. J., Lacy, M., & Martínez-Sansigre, A. 2008a, *MNRAS*, 389, 799

Smith, D. J. B., Jarvis, M. J., Simpson, C., & Martínez-Sansigre, A. 2009, *MNRAS*, 393, 309

Somerville, R. S., Lee, K., Ferguson, H. C., Gardner, J. P., Moustakas, L. A., & Giavalisco, M. 2004, *ApJL*, 600, L171

Steidel, C. C., Adelberger, K. L., Dickinson, M., Giavalisco, M., Pettini, M., & Kellogg, M. 1998, *ApJ*, 492, 428

Steidel, C. C., Adelberger, K. L., Shapley, A. E., Pettini, M., Dickinson, M., & Giavalisco, M. 2000, *ApJ*, 532, 170

Steidel, C. C., Adelberger, K. L., Shapley, A. E., Pettini, M., Dickinson, M., & Giavalisco, M. 2003, *ApJ*, 592, 728

Taniguchi, Y., & Shioya, Y. 2000, *ApJL*, 532, L13

Villar-Martín, M. 2007, *New Astronomy Review*, 51, 194

Weidinger, M., Møller, P., & Fynbo, J. P. U. 2004, *Nature*, 430, 999

Yang, Y., Zabludoff, A. I., Davé, R., Eisenstein, D. J., Pinto, P. A., Katz, N., Weinberg, D. H., & Barton, E. J.

2006, *ApJ*, 640, 539

Yang, Y., Zabludoff, A., Tremonti, C., Eisenstein, D., & Davé, R. 2009, *ApJ*, 693, 1579

APPENDIX A: THE LY α BLOB LUMINOSITY FUNCTION IN AN OVERDENSE REGION

Steidel et al. (1998) found an overdensity of $\delta_{\text{LBG}} = 5.0 \pm 1.2$ Lyman Break Galaxies (LBGs Steidel et al. 2003) per unit volume within their survey volume of $V_s \sim 0.15 \times 10^5 \text{ cMpc}^3$. This highly overdense region is contained within the approximately nine times larger volume, V_s (the subscripts 's' and 'S' refer to the smaller and larger survey volumes, respectively), in which the Ly α blobs were found (Matsuda et al. 2004). In later work, Matsuda et al. (2005) found that the Ly α blobs populate a region of our Universe that contains three filaments. These filaments intersect right where Steidel et al. Steidel et al. (1998) found their enhanced population of LBGs. Therefore, the survey volume that was probed by Matsuda et al. (2004) is overdense, but not as much as the 'sub-volume' that was probed originally by Steidel et al. (2000). Indeed, Matsuda et al. (2005) found that the number density of Ly α emitters in the filaments – and therefore the volume originally probed by Steidel et al. (1998, 2000) – is approximately two to three times higher than the average number density within their entire volume. If we assume that the LBG overdensity is suppressed by a similar factor, then this implies that the overall survey volume of Matsuda et al. (2004) contains $\sim (6.0 \pm 1.2)/3 \sim 2.0 \pm 0.4$ more LBGs than average.

LBGs populate dark matter halos of mass $m = 10^{11.8} M_\odot$ (Adelberger et al. 2005), which are biased tracers of the overall mass density field. Therefore, we convert the LBG overdensity, $\delta_{\text{LBG}} = 1.0 \pm 0.4$ into an overall matter overdensity through $\delta_{\text{LBG}} = b_{\text{LBG}} \delta_{\text{M}}$, in which $b_{\text{LBG}} \sim 3.0$ is the linear bias parameter of dark matter halos hosting the LBGs (Sheth et al. 2001). We therefore find that $\delta_{\text{M}} = 0.3 \pm 0.1$, which corresponds to $\delta_{\text{M}} = (3 \pm 1) \times \sigma(V_s)$. This result corresponds to the range of overdensities that was used⁷ in this paper.

⁷ Lidz et al. (2007) compute the differential probability that a point is at an overdensity δ_R when smoothed on a scale R , given that it is at an overdensity δ_r when smoothed on a smaller scale r , $P(\delta_R, \sigma_R | \delta_r, \sigma_r)$ (see their Eq. 4). For a bias parameter $b_{\text{LBG}} = 3.0$ we find that the mass overdensity within the survey volume of Steidel et al. (1998) is $\delta_{\text{M,r}} = \frac{\delta_{\text{LBG}}}{b_{\text{LBG}}} = 1.7 \pm 0.4 = (6.0 \pm 1.5) \times \sigma(V_s)$. Here, the subscripts 'r' and 'R' refer to the smaller and larger survey volumes, respectively. Using the expression of Lidz et al. (2007) we find that $\delta_{\text{M,R}} = (6.0 \pm 1.5) \times \sigma(V_s)$ translates to $\delta_{\text{M,R}} = (3.3 \pm 0.8) \times \sigma(V_S)$. This procedure therefore gives us an estimate of the overdensity that is consistent with our estimate based on the number of observed LBGs and Ly α emitting galaxies.